

Morphodynamic Impact of Sea Breeze Activity on a Beach with Beach Cusp Morphology

Gerhard Masselink and Charitha Pattiaratchi

Centre for Water Research
University of Western Australia
Nedlands, Western Australia 6907

ABSTRACT

MASSELINK, G. and PATTIARATCHI, C., 1998. Morphodynamic impact of sea breeze activity on a beach with beach cusp morphology. *Journal of Coastal Research*, 14(2), 393-406. Royal Palm Beach (Florida), ISSN 0749-0208.



Beach morphology and nearshore hydrodynamics were monitored over a number of sea breeze cycles on a beach with pronounced beach cusp morphology in southwestern Australia. The action of the sea breeze resulted in consistent changes to the incident wave field and beach cusp morphology, and induced a diurnal cycle of beach change. The morphological changes were accomplished without an apparent sediment gain or loss, but involved a redistribution of sediment within the cusp morphological system.

During the sea breeze, the addition of locally-generated, short-period wind waves to the background swell resulted in an increase in wave height, a decrease in wave period and an intensification of the nearshore currents. The cusp morphology became increasingly subdued due to accretion in the embayment and, to a lesser extent, erosion of the horns. After the cessation of the sea breeze, the wind-wave energy level gradually decreased and the associated wind-wave period increased. Accretion on the cusp horns was accompanied by minor erosion of the embayment and resulted in an accentuation of the cusp morphology. The build-up of the cusp morphology was a consequence of the morphodynamic feedback between the antecedent cusp morphology and the wave runup characteristics. The wave runup was diverted from the horn into the embayment, resulting in decreased backwash volumes and hence build-up of the horn. In the cusp embayment, increased backwash volumes resulted in scouring and the suppression of potential swash events at the base of the beachface. Consequently, the proportion of infragravity-wave energy in the runup record was larger in the embayment than on the horn.

Ten hours after the sea breeze had stopped blowing, significant amounts of wind-wave energy were still present. It is suggested that these wind waves were generated a distance of almost 200 km south of the study area, implying that the presence of the local sea breeze may have regional implications for coastal processes.

ADDITIONAL INDEX WORDS: *Beach morphology, wind waves, beach cusp coastal processes.*

INTRODUCTION

On microtidal, wave-dominated beaches, morphological change is primarily induced by variations in the incident-wave climate. These variations are usually ascribed to the passage of storms. An often neglected source of changes to the incoming wave field is the diurnal sea breeze. The impact of sea breeze activity on beaches is often obscured by the presence of high-wave energy levels or large tidal ranges, and there has been the tendency to discount its effects on coastal processes. Whereas the meteorological aspects of the diurnal sea breeze have been studied extensively (HSU, 1988; SIMPSON, 1994), very little attention has been devoted to the effects of sea breeze activity on the nearshore environment.

INMAN and FILLOUX (1960) monitored morphological changes on a low-wave energy, macrotidal beach in the Gulf of California. In this region, the high water of spring tides occurs during the early afternoon when the sea breeze regime is strongest. The coincidence of maximum wave intensity with spring high tide results in the overtopping and erosion of the beach berm, and sediment deposition on the lower part of the intertidal profile. This phase-coupling between the tide

and the sea breeze induces a fortnightly cycle of erosion and deposition of the beach. INMAN and FILLOUX (1960) measured sea breezes that blew onshore with maximum wind speeds of up to 7.5 m/sec. Sea breeze-generated waves had heights of 0.6 m and periods of 5 sec (visual estimates). After the cessation of the sea breeze, the wave height decreased rapidly and fell to pre-sea breeze values within several hours.

SONU *et al.* (1973) conducted a comprehensive study of sea breeze effects on coastal processes along the Gulf of Mexico. The sea breeze usually started between 10:00 and 11:00 hrs, attained maximum wind velocities of 5-6 m/sec around 13:30 hr and subsided between 14:00 and 20:00 hr. The strongest winds during the sea breeze typically made an angle of 30° with the line normal to the shoreline. During a diurnal sea breeze cycle, the significant wave height increased from 0.2-0.3 m in the morning to 0.5-0.6 m at the end of the afternoon and then decreased overnight. The average wave period changed each day from 4-5 sec in the morning to 2-3 sec in the afternoon and then gradually increased overnight to the morning maximum. The wind waves generated by the sea breeze approached the shoreline under a 30-40° angle and produced a high-frequency peak in the nearshore wave spectrum that dominated the background swell in the afternoon and evening. Part of the wind-wave energy persisted over-

night and was present until the initiation of a new sea breeze cycle the next morning. SONU *et al.* (1973) also noted the impact of the sea breeze on nearshore currents. Prior to the sea breeze, closed nearshore cell circulation prevailed, characterised by longshore feeder currents and seaward-returning rips. As the wave characteristics and incidence angles changed in response to the sea breeze, the closed cell circulations were broken up and replaced by longshore meandering currents. Wind-driven currents were measured outside the surf zone during the sea breeze.

PATTIARATCHI *et al.* (1997) and MASSELINK and PATTIARATCHI (1996a) discuss the results of a field survey conducted in southwestern Australia. Winds generated by the sea breeze had velocities exceeding 10 m/sec and resulted in an almost instantaneous transformation of the incoming wave field and sediment transport processes. During the sea breeze, the root mean square wave height increased from 0.3 to 0.5 m whereas the zero-downcrossing period decreased from 8 to 4 sec. Around the mid-surf zone position, offshore-directed mean flows increased from almost zero to 0.15 m/sec and longshore current velocities increased from 0.05 m/sec to 1 m/sec. The amount of suspended sediment in the water increased six-fold and the longshore suspended sediment transport rate across the surf zone increased by a factor of one hundred. In turn, the changes in the hydrodynamic conditions induced an adjustment of the beach morphology: up to half a meter of erosion occurred on the upper part of the beach within 30 minutes, whereas deposition took place on the lower part. Beach cusp morphology was eradicated during the sea breeze, but reformed overnight. Monitoring was limited to part of the sea breeze cycle as energetic surf zone conditions encountered during the sea breeze resulted in the toppling over and/or burial of the instruments. MASSELINK and PATTIARATCHI (1996a) concluded that the effect of strong sea breeze activity on nearshore processes is similar to that of a medium-size storm.

Apart from the four above-mentioned investigations, no studies have been reported in the literature regarding the impact of sea breeze activity on coastal processes. This is surprising because tropical and subtropical regions, where the sea breeze is known to occur for at least part of the year, occupy at least two thirds of the earth's surface. As pointed out by SONU *et al.* (1973), even in areas of modest sea breeze intensity, the long-term effect of repetitive sea breeze excitation can be dramatic. For example, along the low-wave energy, sea breeze-dominated part of the southwestern Australian coastline, sediment moves northward in the summer due to the sea breeze and is transported southward during winter storms (PATTIARATCHI *et al.*, 1997). The sea breeze is therefore of fundamental importance for the sediment budget of the region.

The principal aim of this paper is to investigate the morphodynamic effects of the sea breeze on beaches, *i.e.*, the impact of sea breeze activity on the beach morphology, the hydrodynamic processes, and their mutual interactions. Beach morphology and hydrodynamics were monitored continuously over five days on a beach with pronounced beach cusp morphology in southwestern Australia. The data include three complete sea breeze cycles, and in particular, the temporal

changes that occurred to the beach cusp morphology under the influence of sea breeze activity are discussed.

FIELD TECHNIQUES

The field survey was conducted from 03/03/95 to 09/03/95 on City Beach, a steep-gradient (5–6°), low-wave energy, microtidal beach in Perth, Western Australia (Figure 1). The beachface of City Beach consists of medium-sized sand ($D_{50} = 0.3\text{--}0.5$ mm) and is typically characterised by pronounced beach cusp morphology. During the survey, data were collected on: (1) beach morphology; (2) wind speed and direction; (3) instantaneous shoreline; and (4) nearshore water surface elevation, current velocity and suspended sediment concentration. In addition, offshore wave and tide data were obtained from the Department of Transport, Western Australia.

At the start of the survey period, pronounced beach cusp morphology was present with a spacing of 30 m and the experimental design was dictated by the beach morphology. Seven transects with a spacing of 7.5 m were established across the beach, with the primary transect located in the centre of the cusp embayment, two lines transecting adjacent cusp horns and four transects located between horn and embayment. Along each transect, twenty steel pegs (8 mm thick and 1 m long) were inserted in the beach at 1 m intervals, extending from the top of the berm to the base of the beachface (Figure 2). All pegs were installed above MSL. The sand surface adjacent to the pegs and the beach profile beyond the seaward-most peg were surveyed every morning using an electronic theodolite (TOPCON). These measurements were related to a temporary benchmark. The height of the top of the pegs above the sand surface was measured every hour by a group of volunteers. Bed elevation changes in the form of accretion/erosion often threatened to bury/expose the steel pegs. In these instances, the pegs were "reset" by pulling up or hammering in. To enable continuation of the data record, the height of the peg above the sand surface was measured before and after resetting.

Wind speed and direction were measured using a standard weather station deployed at 5 m height, just landward of the berm at the southern end of the survey area. The data were block-averaged over 10 minutes and recorded using a data logger. The instantaneous shoreline was measured from 12:30 hr on 08/03/95 until 10:30 hr on 09/03/95 using dual-wire, resistance runup gauges (HOLMAN and GUZA, 1984). Three runup wires were deployed simultaneously; two across cusp embayments and one transecting the cusp horn. The runup gauges were deployed with the seaward end of the wire located just beyond the lower swash zone. The shoreward end of the wire was located on the berm crest and connected to a computer. The 25 m long runup gauge was mounted across the beachface using a series of fibreglass mounting brackets attached to wooden stakes. The mounting brackets could easily be adjusted in accordance with fluctuations in the sediment level and the resistance wires were kept at a constant elevation of 0.02–0.03 m above the bed. This required continuous monitoring of the runup wires over 22 hours which was a very tiring and arduous task. Data were re-

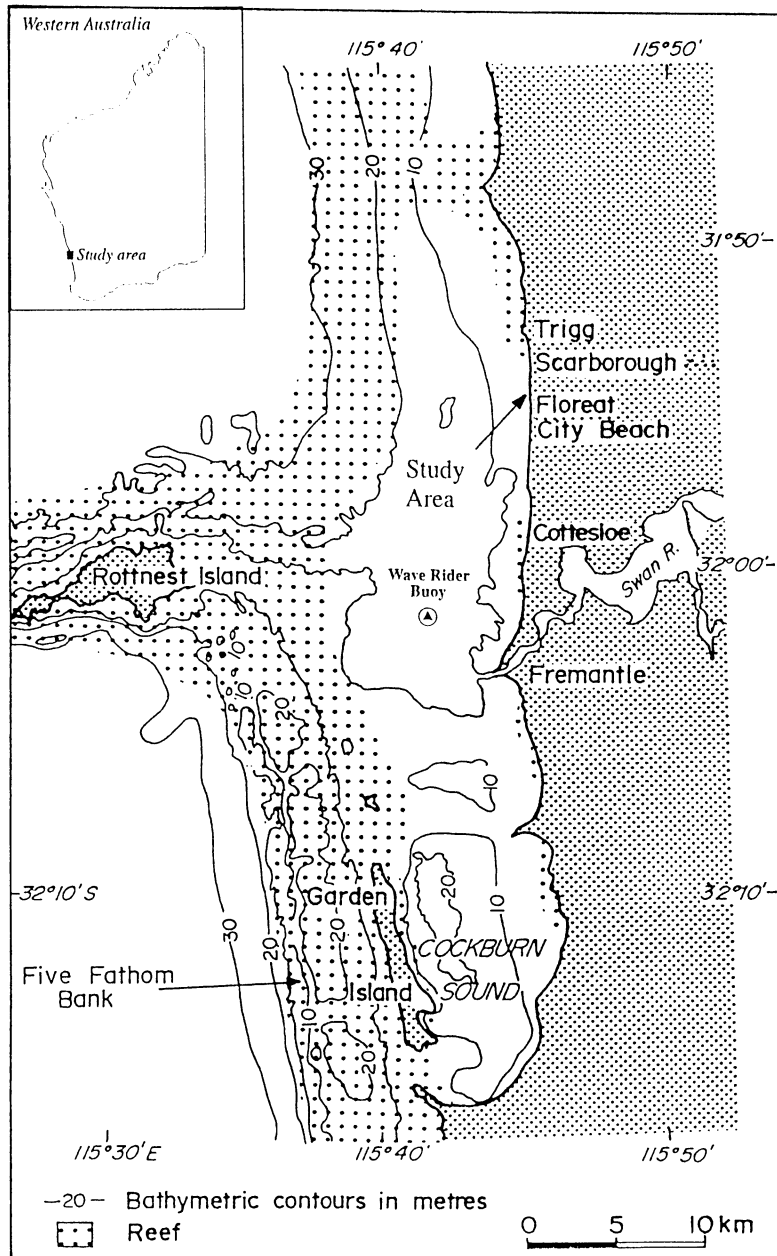


Figure 1. Location of the study area.

corded continuously at 2 Hz and stored on a computer. Data on nearshore waves, currents and suspended sediment concentrations were collected using the "S-probe", an instrument package consisting of a pressure sensor, an acoustic current meter and three optical backscatterance (OBS) sensors. Data collected by the OBS sensors will not be discussed here, but are reported elsewhere (MASSELINK and PATTIARACHI, 1996b). The pressure sensor was mounted 0.35 m from the sea bed, whereas the two-dimensional, horizontal current velocity was recorded 0.2 m above the bed. The S-probe was deployed opposite the cusp

embayment in 1.3–1.7 m of water, approximately 20m from the shoreline (Figure 2). Throughout the survey period, the S-probe was located just outside the surf zone, with only occasional wave breaking occurring over the probe. The data were recorded via a cable connected to a shore-based computer and were logged at 2 Hz. Deep water wave data were collected offshore Fremantle in 17 m water depth (10 km south of City Beach; Figure 1). Data were sampled at 1 Hz and wave statistics were calculated every 20 minutes. Tidal water levels were measured every 2 minutes in the Fremantle Harbour (Figure 1).

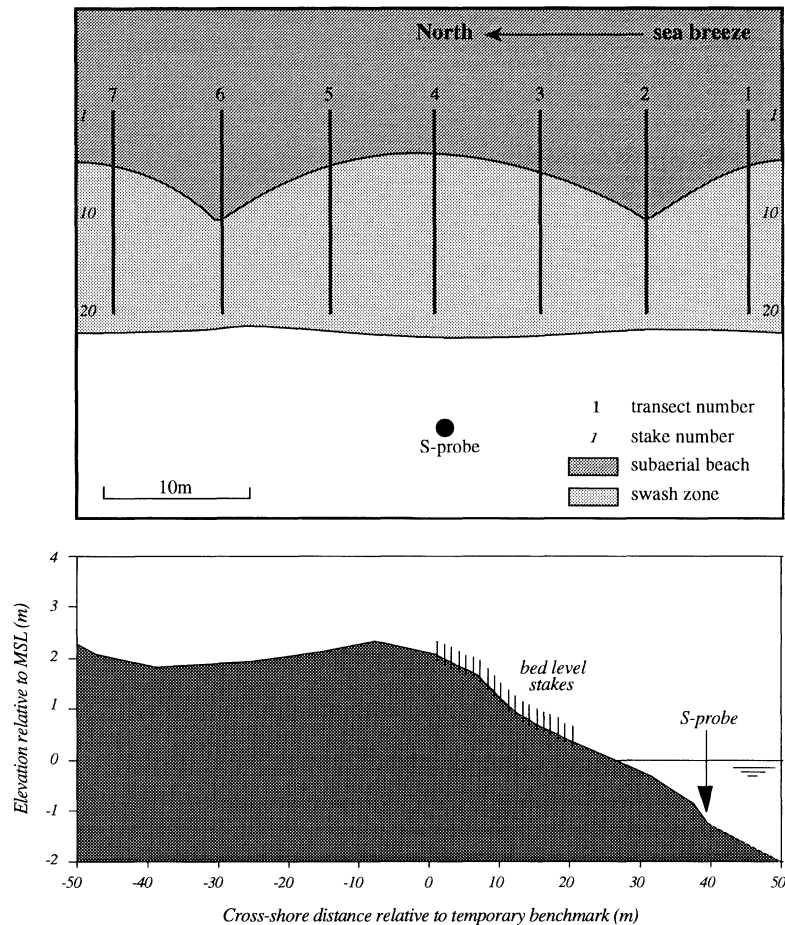


Figure 2. Beach profile of City Beach and location of bed elevations rods and the S-probe. The beach profile was measured through the centre of the cusp embayment.

ANALYSIS TECHNIQUES

By combining and cross-checking survey data with peg data, an hourly time series of the three-dimensional beach (cusp) morphology was obtained over the complete survey period. An extensive error analysis was carried out (FEAVER, 1995), and the overall accuracy of the bed elevation measurements is considered better than ± 0.03 m. The bed elevations were transferred to mean sea level (MSL) using the mean water depth over the survey period obtained with the S-probe. The morphological data were used to compute the amount of sediment contained in the survey area above MSL. Because all pegs were installed above MSL, the total sediment volume was simply determined by multiplying the bed elevation at each peg with a surface area of 1 m by 7.5 m, and subsequently summing the individual peg volumes. To calculate the sediment volume per unit meter beach width over a transect, the bed elevations of all the pegs in that transect were summed. A quantitative measure of the prominence of the three-dimensionality of the beach morphology was obtained using trend surface analysis. A first-order trend surface (*i.e.*, a planar surface) was fitted to the beach mor-

phological data following DAVIS (1986). Subsequently, the correlation coefficient (r^2) was computed to determine the goodness of fit. Inspection of the data indicated that r^2 decreases as beach cusps become more developed and vice versa. Relatively smaller correlation coefficients ($r^2 < 0.95$) are indicative of pronounced beach cusp morphology, whereas larger correlation coefficients ($r^2 > 0.98$) were obtained in case of a planar beach.

The wave run-up wires were calibrated *in situ* in the field before and after deployment by shorting the wire at known locations. The "horizontal runup" was converted to "vertical runup" using the beach profile measured at the location of the runup wires prior to the collection of runup data. The acoustic current meter was calibrated in a flume. The manufacturer's instructions were followed for the calibration of the weather station and pressure sensor. Statistical analysis of the time series of water-surface elevation, current velocity, suspended sediment concentration and instantaneous shoreline were carried out on time series of 2,048 points. For a sample frequency of 2 Hz this implies a length of the time series of just over 17 minutes. The root mean square (rms)

trough-to-crest wave height and the zero-downcrossing wave period were computed from the high-pass filtered time series (cut-off frequency 0.05 Hz) of the water-surface elevation. The offshore wave heights provided by the Department of Transport were significant wave heights. To facilitate comparison with nearshore wave data, the offshore significant wave heights were converted to rms wave heights using a conversion factor of $1/\sqrt{2}$ (THORNTON and GUZA, 1983).

Using spectral techniques, the individual contributions of different frequency bands to the total amount of variance within a time series were computed and expressed as a percentage. Three main frequency bands were considered: 1) the infragravity-wave band ($f = 0.005\text{--}0.05$ Hz); 2) the swell-wave band ($f = 0.05\text{--}0.15$ Hz); and 3) the wind-wave band ($f = 0.15\text{--}0.5$ Hz). The swell-wave and the wind-wave band collectively made up the incident-wave band. The rms wave height for each of these frequency bands was calculated using $H_{rms} = \sqrt{8\sigma^2}$, where σ^2 is the variance associated with the appropriate frequency band. Autospectral analysis was performed on detrended and Hann-tapered time series of length $N = 2,048$ using the Fast Fourier Transform. The variability of the spectral estimates was reduced by averaging estimates over adjacent frequency bins (MARPLE, 1987). Sixteen adjacent bins were averaged, resulting in 32 degrees of freedom and a frequency-bin width of 0.0156 Hz. The angle of wave incidence was determined using cross-spectral analysis between water surface elevation and current velocity (SHERMAN and GREENWOOD, 1986). The calculated wave angles are subject to a relatively large error range. Misalignment of the S-probe with respect to the shoreline and shortcomings of the technique itself may have resulted in an error margin of $\pm 10^\circ$.

EVENT SUMMARY

Time series of tide level, wind speed and direction, rms offshore wave height, beach sediment volume and trend surface correlation coefficient are plotted in Figure 3 over the survey period (12:00 hr on 03/03/95 until 12:00 hr on 09/03/95). Three distinct periods may be identified:

- (1) **Storm period** (12:00–22:00 hr on 03/03/95). Moderately strong southerly winds with speeds between 5 and 10 m/sec prevailed during this period. The strong winds are considered to be the result of the superposition of the local sea breeze and the regional weather situation. Waves were generated with deep water rms heights in excess of 1 m. The “storm” lasted half a day and the obliquely-incident waves resulted in considerable beach erosion. Approximately 200 m³ of sediment was removed from the beachface, equating to a mean lowering of the bed level of 0.2 m. Beach erosion was concentrated at the location of the cusp horns, resulting in the near-destruction of the beach cusp morphology, as indicated by the increase in the trend surface correlation coefficient from 0.95 to 0.99. The cusp morphology was preserved only in the highest region of the beachface, albeit faintly.
- (2) **Calm weather period** (22:00 hrs on 03/03/95 until 12:00 hr on 06/03/95). Wind velocities dropped to around 3 m/sec and the wind direction shifted towards the east (off-

shore winds). Incident-wave energy gradually reduced with deep water rms wave heights smaller than 0.25 m at the end of the calm weather period. Sediment was returned to the beach and cusp morphology was re-established during this period of decaying wave energy, as demonstrated by a decrease in the trend surface correlation coefficient from 0.99 to 0.93.

- (3) **Sea breeze period** (12:00 hr on 06/03/95 until 12:00 hr on 09/03/95). Three sea breeze cycles occurred in this period with winds blowing from the south with speeds of around 6 m/sec. Prior to the start of the sea breeze, weak easterly winds prevailed and rms wave heights were generally less than 0.2 m. The sea breezes started blowing in the early afternoon, increased in intensity throughout the day, and persisted until the evening. During the afternoon, the wave-energy level progressively increased, attaining maximum deep water rms heights of around 0.4 m early in the evening. Concurrent with the slackening of the sea breeze, the incident-wave height gradually decreased throughout the night. By early morning, wave conditions were back to pre-sea breeze levels. Over the three-day sea breeze period, minor fluctuations occurred in the beach sediment volume and the prominence of the beach cusp morphology.

The destruction and reformation of the beach cusp morphology that took place during the storm and calm weather period respectively are of considerable interest, but will be discussed in a separate submission elsewhere (MASSELINK *et al.*, 1996). The present analysis will focus on the morphodynamic changes that have occurred during the three successive sea breeze cycles.

MORPHODYNAMIC CHANGES OVER A SEA BREEZE CYCLE

Three complete diurnal sea breeze cycles were monitored over the field survey period. During each of these, the onset of the sea breeze was around 13:45 hr and the sea breeze ceased blowing at approximately 20:45 hr. Average wind velocities during the sea breezes were of the order of 5–6 m/sec. Such wind speeds are characteristic of sea breezes that are experienced late in the summer season (March). Stronger sea breezes with speeds up to 15 m/sec are typical during January/February (PATTIARATCHI *et al.*, 1997). The hydrodynamic changes that occurred over the three sea breeze cycles were very similar (Table 1). Those pertaining to the last sea breeze cycle (12:00 hr 08/03/95 to 12:00 hr 09/03/95) will be presented in detail.

The hydrodynamic data represent 17 minute averages and were collected with the S-probe in an average water depth (h) of 1.5 m. However, significant water level changes occurred due to the diurnal tide. High tide was around 12:00 hr on 08/03/95 ($h = 1.7$ m), whereas low tide occurred around 3:00 hr 09/03/95 ($h = 1.3$ m). The tidal modulation of the nearshore water level has to some extent affected the hydrodynamic measurements. For example, during low tide, waves measured by the S-probe were in a more advanced stage of shoaling than during high tide, resulting in larger crest-to-trough wave heights. Nevertheless, the hydrodynamic

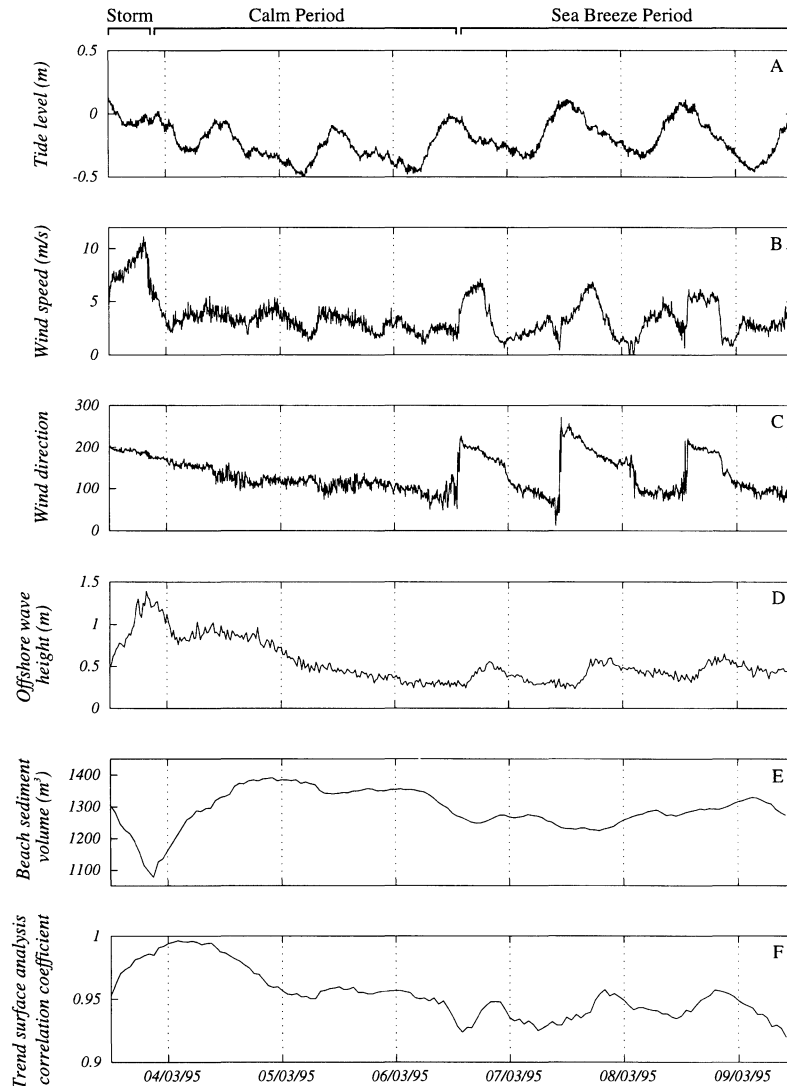


Figure 3. Simultaneous time series of: (A) tide level; (B) wind speed; (C) wind direction; (D) root mean square offshore wave height; (E) beach sediment volume and; and (F) trend surface correlation coefficient over the survey period from 12:00 hr on 03/03/95 to 12:00 hr on 09/03/95.

changes that occurred from 12:00 hr 08/03/95 to 12:00 hr 09/03/95 are predominantly attributed to the diurnal sea breeze cycle.

Wind

Prior to the sea breeze, offshore winds prevailed with speeds of 2–3 m/sec. At 13:45 hr, the sea breeze started, indicated by an abrupt change in the wind direction from east to south and a concomitant increase in the wind velocity (Figure 4). Because the beach has a north–south orientation, the sea breeze blew parallel to the beach. The shore-parallel nature of the Perth sea breeze is the result of the superposition of the regional weather pattern and the local sea breeze system (PATTIARATCHI *et al.*, 1997). The sea breeze persisted for approximately 7 hours and a relatively constant wind speed of 5–6 m/sec was maintained throughout this period. Around

20:45 hr, the sea breeze stopped blowing. The wind direction gradually shifted back to the east and the wind velocities dropped below 4 m/sec. Typically, the onset of the sea breeze is indicated by an abrupt shift in the wind direction, whereas the cessation of the sea breeze is characterised by a gradual change in the wind direction.

Waves

After the onset of the sea breeze, almost immediate changes occurred to the incoming wave field. During the sea breeze, the rms wave height increased from 0.25 to 0.4 m, whereas the wave period decreased from 9 to 5 sec (Figure 5A, B). After the sea breeze, the wave height remained relatively constant. The wave period, however, started increasing as soon as the sea breeze had subsided. Around 6:00 hr the next morning, *i.e.*, 9 hours after the end of the sea breeze,

Table 1. Summary of hydrodynamic conditions during the sea breeze.

	Sea Breeze 1	Sea Breeze 2	Sea Breeze 3	Swell-waves
Background conditions				
Start sea breeze	13:45 hrs	13:45 hrs	13:45 hrs	
End sea breeze	20:45 hrs	20:45 hrs	20:45 hrs	
Max. wind speed	6.5 m/s	6.5 m/s	5.5 m/s	
Mean wind speed during sea breeze	5.5 m/s	5.5 m/s	5 m/s	
Wind direction	220–170°	220–170°	210–180°	
Water depth	1.35–1.75 m	1.35–1.75 m	1.35–1.75 m	
Hydrodynamic conditions				
Max. root mean square wave height	0.5 m	0.4 m	0.45 m	0.3 m
Min. zero-downcrossing wave period	4.5 s	4.5 s	5 s	10 s
Max. mean wave angle	20°	20°	19°	5°
Max. wind-wave angle	32°	32°	32°	10°
Max. % wind-wave energy	55%	60%	50%	10%
Max. offshore bed return flow velocity	0.07 m/s	0.09 m/s	0.07 m/s	0 m/s
Max. s.d. cross-shore current velocity	0.42 m/s	0.45 m/s	0.48 m/s	0.3 m/s
Max. longshore current velocity	0.2 m/s	0.18 m/s	0.15 m/s	0.05 m/s
Max. s.d. longshore current velocity	0.22 m/s	0.22 m/s	0.22 m/s	0.1 m/s

the wave period reached pre-sea breeze levels. The decrease in wave period during the sea breeze is ascribed to the addition of locally-generated, short-period wind waves to the long-period swell waves. This is demonstrated by the temporal variation of the proportion of swell- ($f = 0.05\text{--}0.15$ Hz) and wind-wave energy ($f = 0.15\text{--}0.5$ Hz) in the water surface elevation record (Figure 5C). Prior to the sea breeze, approximately 80% of the water motion in the nearshore zone was at swell-wave frequencies. During the sea breeze, however, the contribution of the wind-wave frequency increased up to 45%, almost equalling the contribution by the swell waves. After the cessation of the sea breeze, the proportion of wind-wave energy gradually decreased, reaching pre-sea breeze values around 2:00 hr. The proportion of infragravity-wave energy ($f = 0.005\text{--}0.05$ Hz) was also computed but did not show any apparent trend over the sea breeze cycle and remained constant at 0.5–2% (not shown).

Wave angles were calculated for wind-, swell- and incident-wave frequencies (Figure 5D). The latter frequency band

ranges from 0.05–0.5 Hz. The incident-wave angle increased from 6° to 18° during the sea breeze, and fell back to 6° at 4:00 hr. The swell-wave angle remained around 6° over the entire day. The wind-wave angle reached values of 30° during the sea breeze and gradually decreased to 5° after the sea breeze. The calculated values for the angle of wave incidence are in agreement with the visual observations.

Currents

The S-probe was located outside the surf zone over the entire sea breeze cycle. Nevertheless, significant mean cross-shore and longshore currents were measured during and after the sea breeze (Figure 6A). Net offshore flows persisted during the sea breeze, with maximum velocities of 0.07 m/sec occurring at the end of the sea breeze period. The offshore-directed mean flow is ascribed to the bed return flow or undertow which, as shown by MASSELINK and BLACK (1995), can extend some distance outside the surf zone. The mean

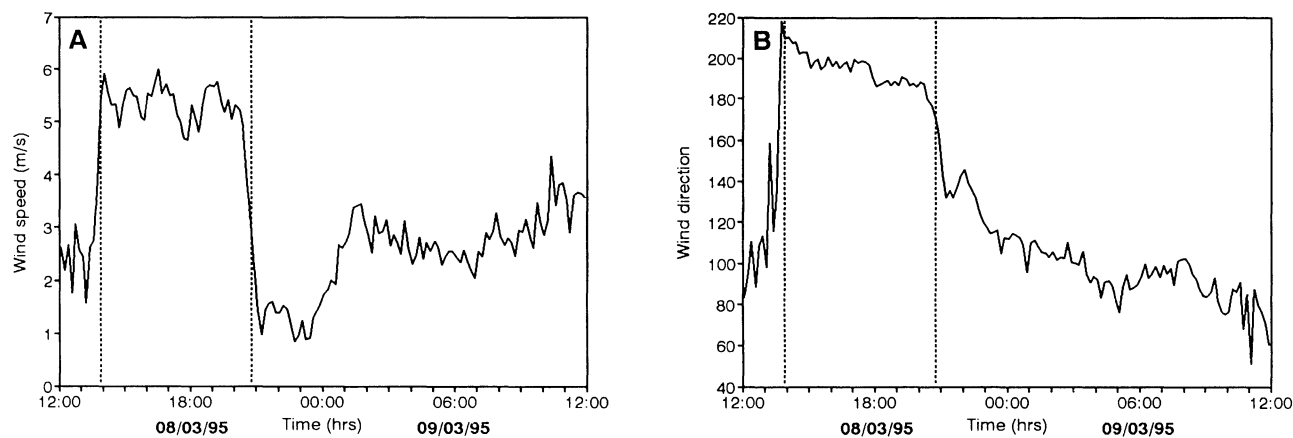


Figure 4. (A) Mean wind velocity and (B) mean wind direction from 12:00 hr on 08/03/95 to 12:00 hr on 09/03/95. The sea breeze period is demarcated by the dashed lines.

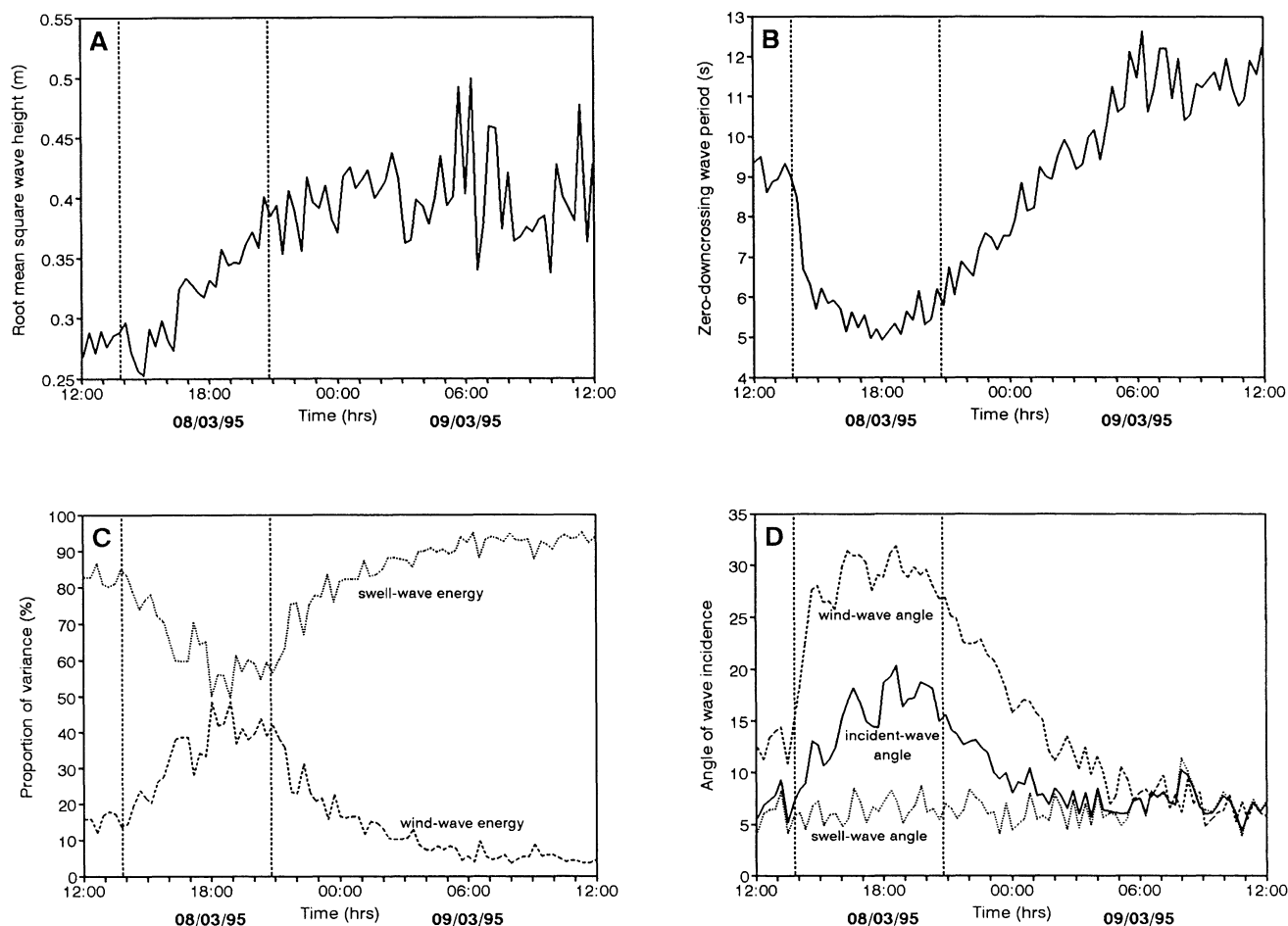


Figure 5. (A) Root mean square trough-to-crest wave height; (B) mean zero-downcrossing wave period; (C) proportion of swell- and wind-wave energy; and (D) angle of wave incidence for wind, swell and incident waves from 12:00 hr on 08/03/95 to 12:00 hr on 09/03/95. The sea breeze period is demarcated by the dashed lines.

cross-shore velocities gradually decreased after the sea breeze had subsided and reached insignificant values around 6:00 hr. The longshore current flowed in a northerly direction with velocities of 0.04 m/sec before and after the sea breeze, and speeds of 0.14 m/sec during the sea breeze. Within several hours after the end of the sea breeze, longshore current velocities dropped to pre-sea breeze values. It is suggested that the mean longshore flow was driven by the waves as well as the wind.

The standard deviation of the cross-shore current velocity record (σ_u) increased during the sea breeze from 0.3 to 0.45 m/sec (Figure 6B). After the sea breeze, σ_u remained relatively constant for several hours, but started decreasing around 2:00 hr. At approximately 6:00 hr, σ_u had fallen to 0.3 m/sec. The standard deviation of the longshore current velocity record (σ_v) increased from 0.1 to 0.22 m/sec during the sea breeze due to the obliquely-incident wind waves. Following the end of the sea breeze, σ_v gradually decreased, reaching a relatively constant value of around 0.14 m/sec at 6:00 hr.

Energy spectra of the cross-shore current were computed to construct a three-dimensional time-frequency plot to illustrate the change in spectral signature over the sea breeze cycle (Figure 7). The cross-shore current data were used, rather than the water surface elevation data because they show more clearly the energy present at wind-wave frequencies ($f > 0.15$ Hz). In addition, cross-shore current velocities are more relevant with respect to sediment entrainment and transport, and ensuing morphological change. The background swell is present in the time-frequency plot in the form of a linear ridge at frequency 0.07–0.1 Hz. The peak period associated with the swell-wave energy was 12 sec and remained relatively constant. The amount of swell-wave energy increased marginally during the sea breeze. However, it is not possible to assess whether this increase is related to some sort of energy transfer from the sea breeze-generated wind waves to the swell waves (SONU *et al.*, 1973), or to the reduced water depths due to low tide conditions. After the onset of the sea breeze (14:00 hr), wind-wave energy starts to emerge at the high-frequency end of the spectra, indicating

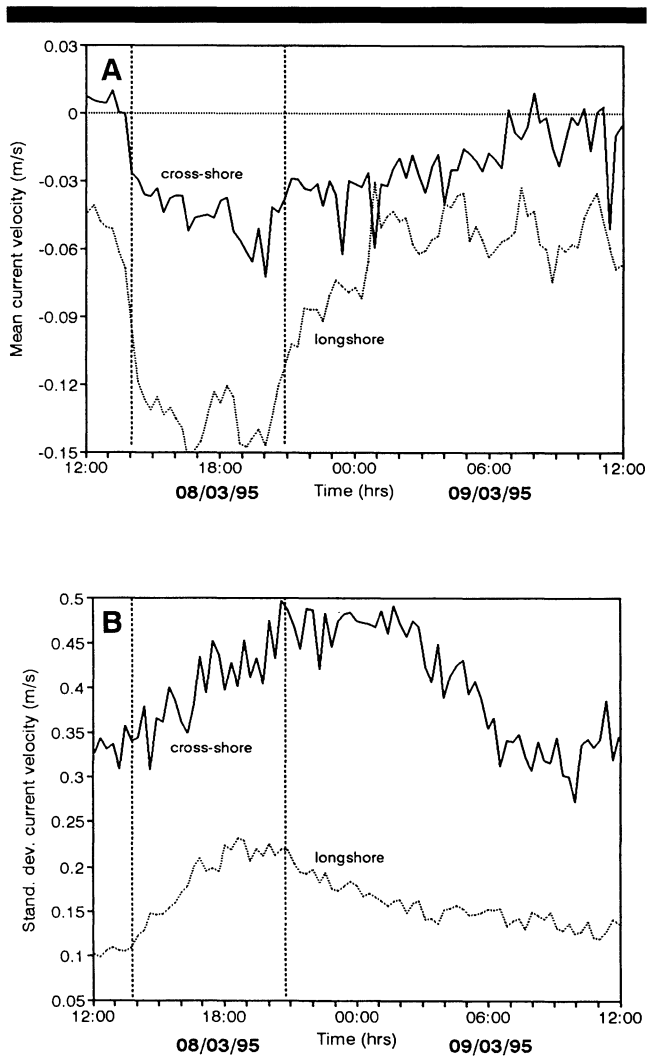


Figure 6. (A) Mean cross-shore and longshore current velocity and (B) standard deviation of the cross-shore and longshore current velocity from 12:00 hr on 08/03/95 to 12:00 hrs on 09/03/95. The sea breeze period is demarcated by the dashed lines.

peak wave periods of 2.5 sec. During the sea breeze, the frequency associated with the wind waves decreased progressively, forming a curving ridge in the frequency-time plot. At the end of the sea breeze (21:00 hr), the wind-wave energy was concentrated around a frequency of 0.25 Hz, indicating a peak period of 4 sec. After the sea breeze has subsided, the wind-wave energy gradually decreased, but remained significant. The frequency associated with the wind-wave energy decreased to 0.15 Hz, merging with the swell-wave energy.

A contour diagram of the cross-shore current spectra collected over three consecutive sea breeze cycles illustrates more clearly the temporal variation in the spectral shape of the cross-shore flow field (Figure 8). Over all three 24 hour periods, the narrow-banded swell peak remained at a constant frequency of around 0.085 Hz. Wind-wave energy starts appearing immediately after the onset of the sea breeze and

the evolution of the wind-wave frequency is similar for all three sea breeze cycles.

Runup

The instantaneous shoreline was measured continuously for almost 22 hours from 12:30 hr on 08/03/95 until 10:30 hr on 09/03/95 in the cusp embayment south of the survey line (4 m south of transect 1), on the cusp horn (2 m north of transect 2) and in the embayment with the survey line (1 m north of transect 4). Data from both cusp embayments were similar, and only those collected from the northern embayment will be discussed. In contrast to the cross-shore current record, the spectral characteristics of the wave runup on the cusp horn and in the cusp embayment were unaffected by the sea breeze (Figure 9). Insignificant amounts of wind-wave energy are present in the runup spectra and because the sea breeze is primarily manifested in nearshore water fluctuations at the wind-wave frequencies ($f > 0.15$ Hz), the sea breeze is not represented in the runup data. The peak runup period on the cusp horn ranged between 11–14 sec, whereas the swash motion in the embayment was characterised by a peak period of 13–15 sec. The variance in the runup time series collected on the horn was approximately 25% larger than that measured in the embayment; the vertical rms swash excursion on the horn was around 0.65 m, whereas in the embayment the vertical rms swash excursion was approximately 0.5 m.

The runup data collected in the cusp embayment contain significantly more energy at infragravity frequencies ($f < 0.05$ Hz) than those measured on the horn (Figure 9). This is considered a result of the water circulation associated with the cusp morphology. Field observations indicate that part of the wave runup on the horn is diverted into adjacent cusp embayments. Consequently, the backwash volume in the embayments is larger than the uprush volume. This results in the suppression of a large number of potential uprush events at the base of the beachface and the generation of local infragravity energy. In contrast to the findings of PATTIARACHI *et al.* (1997), who demonstrated that before the sea breeze, the amount of infragravity energy in the runup record was significantly larger than during the sea breeze, the proportion of infragravity energy remained constant over the sea breeze cycle. Around 10% of the runup motion on the cusp horn was at infragravity frequencies, whereas in the embayment, infragravity motion accounted for 20–30% of the total variance.

Beach Morphology

The three-dimensional beach morphology responded strongly to sea breeze activity (Figure 10). During the sea breeze (14:00–21:00 hr), cusp morphology became increasingly subdued due to accretion in the embayment (+0.25 m) and, to a lesser extent, erosion of the horns (−0.15 m). Field observations indicated that these morphological changes were predominantly induced by obliquely-incident wave runup that swept over the cusp horn into the embayment. These lateral swashes eroded the horn and deposited sediments in the cusp embayment. The changes in the beach morphology

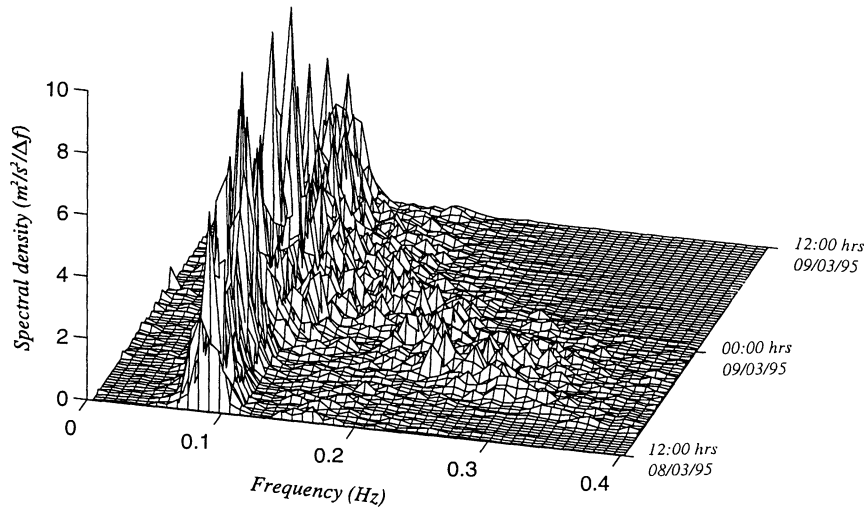


Figure 7. Frequency-time plot of cross-shore current data collected from 12:00 hr on 08/03/95 to 12:00 hr on 09/03/95. The curving ridge in the plot represents sea breeze-generated wind waves.

due to the sea breeze were accomplished without an apparent sediment gain or loss, and involved a redistribution of sediment within the cusp morphological system.

After cessation of the sea breeze (21:00–4:00 hr), accretion on the cusp horns (+0.25 m) was accompanied by minor erosion of the embayment (−0.10 m), resulting in an accentuation of the cusp morphology. The build-up of the cusp morphology was a consequence of the morphodynamic feedback between the antecedent cusp morphology and the wave runup characteristics. Due to the cusp morphology, wave runup was diverted from both horns into the embayment. This led to

reduced backwash volumes on the horns and consequent accretion. In the embayment, the addition of part of the runup from the horns increased the backwash volume, resulting in erosion.

The correlation coefficient (r^2) associated with the planar trend surface fitted to the morphological data was used to quantify the prominence of the beach cusps. An r^2 -value close to unity indicates a planar beach, whereas $r^2 < 0.95$ suggests the presence of pronounced beach cusp morphology. The temporal variation in r^2 clearly responded to sea breeze activity (Figure 11A, B). During the relatively high-energy conditions

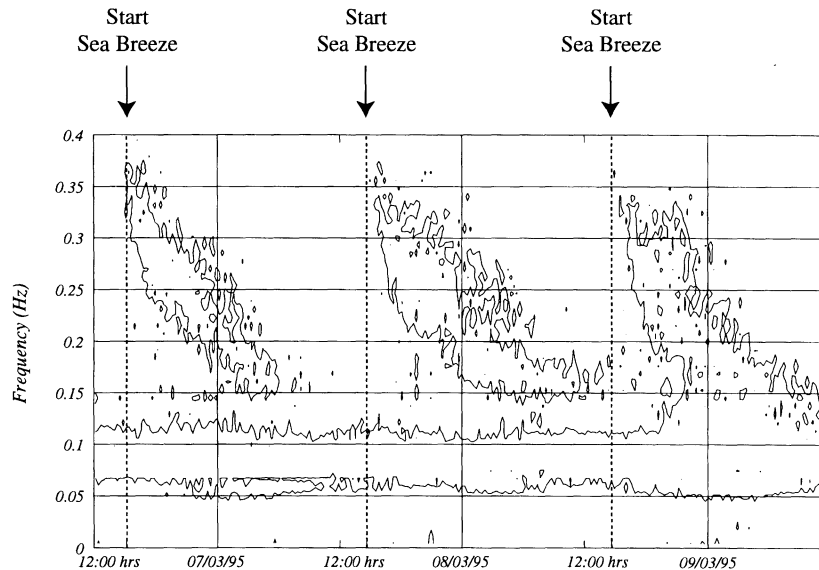


Figure 8. Contour diagram of cross-shore current velocity data collected during three successive sea breeze cycles from 12:00 hr on 06/03/95 to 12:00 hr on 09/03/95. The contour lines represent an energy level of 0.25 m²/sec. The heavy dotted lines indicate the start of the sea breeze (14:45 hr).

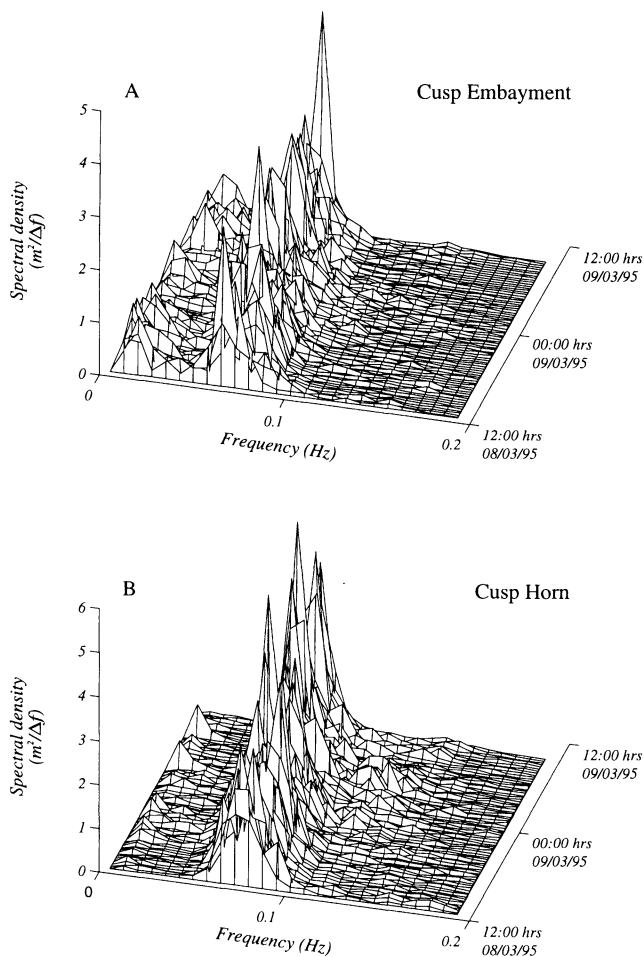


Figure 9. Frequency-time plots of the wave runup on the cusp horn (A) and in the northern cusp embayment (B) from 12:30 hr on 08/03/95 to 10:30 hr on 09/03/95.

of the sea breeze, the flattening of the beach cusps resulted in an increase in r^2 , whereas after the sea breeze, when the wind-wave height is small, cusp build-up is reflected in a decrease in r^2 . Visual observations indicated that the ongoing decrease in r^2 many hours after the cessation of the sea breeze, for example from 4:00–10:00 hr on 09/03/95, was not related to cusp reformation, but to the formation of a small erosion cliff due to rising tide conditions (*cf.* MASSELINK *et al.*, 1996). Cusp build-up generally ceased around 4:00 hr.

No obvious correlation existed between the net changes in the beach sediment volume and the accentuation or planation of the beach cusp morphology (Figure 11B, C). Cusp build-up was usually initiated under net accretionary conditions, but ongoing cusp development occurred under accretionary, eroding and equilibrium conditions. Beach cusp evolution was more related to the reorganization of sediment over the control area. Typically, accentuation of the beach cusps was initiated by cusp horn accretion, followed by embayment erosion (Figure 11D, E). Planation of the cusp morphology was ac-

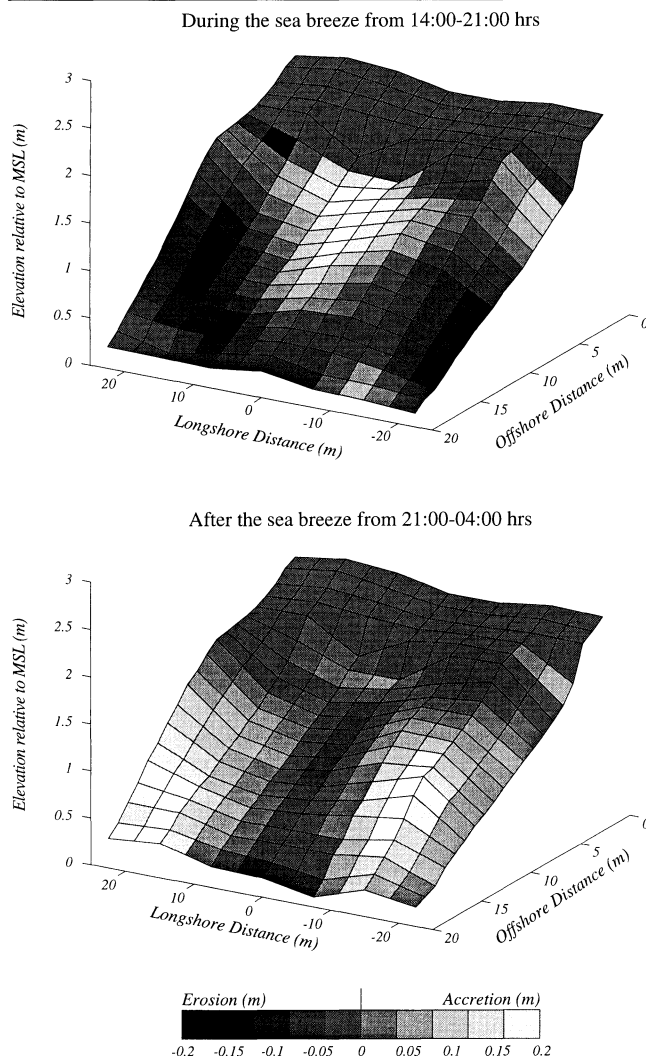


Figure 10. Morphological changes to the beach cusp morphology (A) during the sea breeze from 14:00–21:00 hr on 08/03/95 and (B) after the sea breeze from 21:00 hr on 08/03/95 to 4:00 hr on 09/03/95.

complished by accretion in the cusp embayment, usually occurring prior to erosion of the cusp horn.

The tide provides a confounding factor in the investigation of impact of sea breeze on the beach (cusp) morphology. During all three monitored sea breeze cycles, high tide was just prior to the onset of the sea breeze (Figure 11F). Planation of the cusp morphology due to the sea breeze occurred during the first half of the falling tide, whereas the major part of the cusp build-up took place during the second half of the falling tide. During the rising tide, beach erosion generally occurred, predominantly from the horn, resulting in the planation of the cusp morphology. It may be suggested that the diurnal variation in the beach cusp morphology was partly caused by the diurnal tide, with falling tide conditions promoting cusp build-up and accretionary conditions and rising tide conditions resulting in beach erosion and planation of the cusp

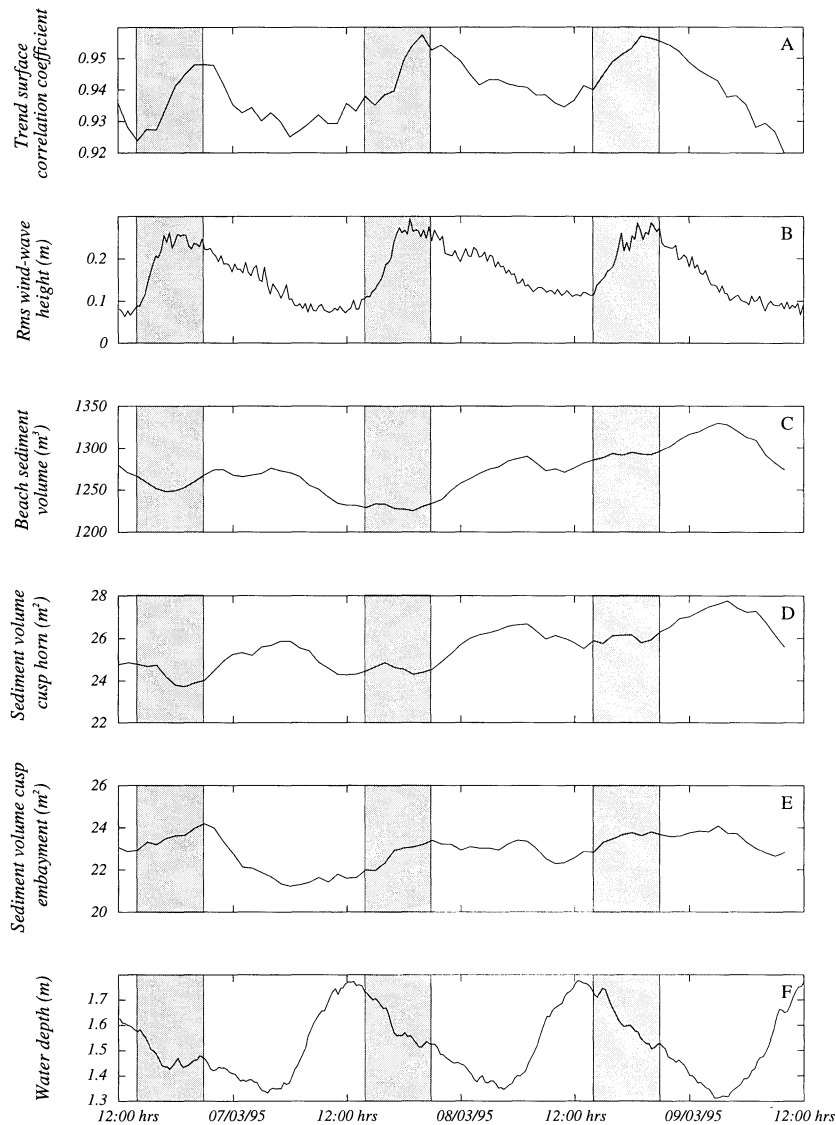


Figure 11. Morphological evolution of the beach cusp morphology during three consecutive sea breeze cycles from 12:00 hr on 06/03/95 to 10:00 hr on 09/03/95: (A) trend surface correlation coefficient; (B) root mean square wind-wave height; (C) beach sediment volume; (D) sediment volume for cusp horn transect; (E) sediment volume for cusp embayment transect; and (F) water depth. The sea breeze period is demarcated by the shaded areas lines.

morphology. However, on 04/03/95, when the sea breeze was absent, no pronounced diurnal cycle of morphological change occurred (Figure 3). It is therefore concluded that morphological variations caused by the tide are of secondary importance compared to those induced by the sea breeze.

DISCUSSION

Wave runup was measured over a sea breeze cycle on the cusp horn and in the cusp embayment. Sea breeze-generated wind waves were not represented in the runup data, confirming that the beachface acts as a low-pass filter to the incident-wave field, allowing only long-period swell waves to reach the upper part of the beach, and filtering out the short-period wind waves (EMERY and GALE, 1951; SONU *et al.*, 1973;

CARLSON, 1984; HEGGE and MASSELINK, 1991). This does not imply, however, that wind waves do not result in wave runup. In the swash zone, the wind waves are "absorbed" by the swell waves by means of swash interactions (HEGGE and ELIOT, 1991), and it is through these interactions that the effects of the sea breeze may be felt. In addition, during the sea breeze, the runup was characterised by a large alongshore component, with swashes sweeping across the cusp horns into the embayments. These lateral swashes were primarily induced by wind waves and were responsible for significant modifications to the nearshore morphology. As a consequence of the beach cusp morphology, alongshore swash motion also occurred prior to the sea breeze under the influence of shore-parallel swell-wave approach. The wave uprush

on the horn was partly diverted into the embayment, as described by BAGNOLD (1940), and resulted in increased backwash volumes in the cusp embayment. Consequently, there was a tendency for the backwash to suppress potential uprush events at the base of the beach face, resulting in the generation of infragravity energy (MASE, 1995).

For many hours after the cessation of the sea breeze, 6 s wind waves were present in the incident-wave field that were clearly related to the sea breeze (Figures 7 and 8). Assuming that these waves represent a "fully developed sea" (PIERSON *et al.*, 1955), their formation requires a wind velocity of 7–8 m/sec, slightly above that recorded on the beach. The deep water wave group celerity of these wind waves is 18 km per hour. Considering that the wind-wave energy is represented in the wave spectra up to 10 hours after the end of the sea breeze, it follows that these waves must have been generated almost 200 km SSE of the study area. Offshore wave spectra computed using data supplied by the Department of Transport and collected some 25 km offshore the study area also indicate the presence of wind-wave energy long after the sea breeze has subsided. Because the seaward extent of the sea breeze is of the order of 50–100 km (SIMPSON, 1994), it follows that such non-locally, sea breeze-generated waves can only occur on coastlines where the sea breeze has a large alongshore component. SONU *et al.* (1973) also measured wind waves long after the cessation of the sea breeze and in their study area (Gulf of Mexico) the sea breeze is also characterised by a large alongshore component.

PATTIARATCHI *et al.* (1997) and MASSELINK and PATTIARATCHI (1996a) suggest that the effect of the sea breeze on nearshore morphodynamics is similar to that of a storm with erosion occurring during the sea breeze by wind waves and recovery taking place between successive sea breezes under the influence of background swell. The continuous morphological measurements suggest, however, that beach recovery in the form of cusp reconstruction, is initiated immediately after the sea breeze has stopped blowing whilst still under the influence obliquely-incident, sea breeze-generated wind waves. In fact, the beach is almost fully recovered to pre-sea breeze conditions at approximately 4:00 hr in the morning, about the time when the "regional" sea breeze waves have finally died out. Only minor morphological changes were accomplished by the background swell waves. This requires us to modify our ideas regarding the supposedly destructive effects of the sea breeze. During the sea breeze, the beach is modified as if under the influence of a mini-storm; beach cusp morphology is planed off and overall beach erosion occurs when the sea breeze is very strong (PATTIARATCHI *et al.*, 1997). Beach recovery, however, starts immediately after the cessation of the sea breeze and is jointly carried out by the wind waves that are forced non-locally by the sea breeze and the background swell.

In contrast to the present results, PATTIARATCHI *et al.* (1997) documented the complete destruction of beach cusp morphology in response to sea breeze activity. However, the latter field investigation experienced mean wind speeds during the sea breeze of 10 m/s, whereas for the three sea breeze cycles reported in the present study the wind velocity did not exceed 7 m/sec. The surf zone conditions experienced during

the field survey of PATTIARATCHI *et al.* (1997) were therefore more energetic, resulting in a more pronounced response of the beach morphology. Interestingly, the medium-size storm that was monitored at the start of the present survey was also characterised by wind speeds up to 10 m/sec, highly energetic surf zone conditions and the complete destruction of the beach cusp morphology (Figure 3).

CONCLUSIONS

The impact of sea breeze activity on coastal processes was investigated through analysis of the morphodynamic changes that occurred over three successive sea breeze cycles along the Perth metropolitan coastline, Western Australia. The present results are site-specific to a certain extent and pertain to relatively strong sea breeze activity with winds blowing predominantly along the shoreline. In many coastal environments that experience sea breeze activity, the associated wind velocities are smaller and directed mainly in the on-shore direction.

The dominant effect of the sea breeze was the generation of obliquely-incident wind waves with rms heights of 0.15–0.25 m and zero-downcrossing periods of 3–6 sec. The addition of these short-period waves to the background swell-wave field resulted in an overall increase in the wave-energy level and a decrease in the wave period. As a consequence, wave-orbital velocities and steady nearshore currents intensified. The hydrodynamic effects of the sea breeze discussed here are similar to those reported by SONU *et al.* (1973), PATTIARATCHI *et al.* (1997) and MASSELINK and PATTIARATCHI (1996a), and re-emphasise the importance of the sea breeze in low-wave energy coastal environments.

The combination of increased nearshore energy levels and oblique wave approach during the sea breeze resulted in the flattening of the beach cusp morphology by means of accretion in the cusp embayment and erosion of the cusp horns. These morphological changes were predominantly induced by obliquely-incident wave runup that swept over the cusp horn into the embayment. These lateral swashes eroded the cusp horn and deposited sediments in the cusp embayment. After the cessation of the sea breeze, cusp morphology was enhanced through accretion on the cusp horns and erosion of the cusp embayment. The changes in the beach morphology due to the sea breeze were accomplished without an apparent sediment gain or loss, and involved a redistribution of sediment within the cusp morphological system.

Wind-wave energy was present in the surf zone long after the sea breeze had ceased to blow. It is inferred that these wind waves were generated a distance of almost 200 km south of the study area by the sea breeze. This implies that the presence of the local sea breeze may have regional implications for coastal processes.

ACKNOWLEDGEMENTS

This project could not have been carried out without the help of a corps of volunteers who, in pairs of two, measured 1680 times how far a steel rod sticks out of the sand. The authors would like to express their sincere thanks for the excellent work they conducted. Additional field assistance

was provided by Ian Eliot, Sheree Feaver and Bruce Hegge. The runup wires were built by Bill Foster. Grant Ryan from the Department of Transport (W.A.) is acknowledged for providing offshore wave and tide data. John Hsu reviewed an early draft of this paper. The morphological data set, consisting of more than 20,000 bed level measurements was expertly collated by Sheree Feaver and is available at request from G.M. This publication has Centre for Water Research reference number ED1061GM.

LITERATURE CITED

- BAGNOLD, R.A., 1940. Beach formation by waves: Some model experiments in a wave tank. *Journal of the Institute of Civil Engineers*, 15, 27–52.
- CARLSON, C.T., 1984. Field studies of run-up on dissipative beaches. *Proceedings 19th International Conference on Coastal Engineering (ASCE)*, 399–414.
- DAVIS, J.C., 1986. *Statistics and Data Analysis in Geology*. New York: Wiley, 646p.
- EMERY, K.O. and GALE, J.F., 1951. Swash and swash marks. *EOS, Transactions American Geophysical Union*, 32, 31–36.
- FEAVER, S., 1995. The Effect of the Sea Breeze on Coastal Processes. Honours Thesis, Department of Environmental Engineering, University of Western Australia (unpublished).
- HEGGE, B.J. and ELIOT, I.G., 1991. Swash interactions on sandy beaches. *Proceedings 10th Australasian Conference on Coastal and Ocean Engineering*, pp. 363–367.
- HEGGE, B.J. and MASSELINK, G., 1991. Groundwater-table response to wave run-up: An experimental study from Western Australia. *Journal of Coastal Research*, 7, 623–634.
- HOLMAN, R.A. and GUZA, R.T., 1984. Measuring run-up on a natural beach. *Coastal Engineering*, 8, 129–140.
- HSU, S.A., 1988. *Coastal Meteorology*. New York: Academic, 260p.
- INMAN, D.L. and FILLoux, J., 1960. Beach cycles related to tide and local wind regime. *Journal of Geology*, 68, 225–231.
- MARPLE, S.L., 1987. *Digital Spectral Analysis with Applications*. Englewood Cliffs, New Jersey: Prentice-Hall, 492p.
- MASE, H., 1995. Frequency down-shift of swash oscillations compared to incident waves. *Journal of Hydraulic Research*, 33, 397–411.
- MASSELINK, G. and BLACK, K.P., 1995. Magnitude and cross-shore structure of bed return flow measured on natural beaches. *Coastal Engineering*.
- MASSELINK, G. and PATTIARATCHI, C., 1996a. The effect of sea breeze on beach morphology, surf zone hydrodynamics and sediment resuspension. Submitted to *Marine Geology*.
- MASSELINK, G. and PATTIARATCHI, C., 1996b. Sediment resuspension outside the surf zone under wind-waves and swell-waves. Submitted to *Sedimentology*.
- MASSELINK, G.; HEGGE, B.J., and PATTIARATCHI, C., 1997. Destruction, formation and modification of beach cusps. *Earth Surface Processes and Landforms* (in press).
- PATTIARATCHI, C.; HEGGE, B.; GOULD, J., and ELIOT, I.G., 1997. Impact of sea breeze activity on nearshore and foreshore processes in Southwestern Australia. *Continental Shelf Research* (in press).
- PIERSON, W.J.; NEUMANN, G., and JAMES, R.W., 1955. *Observing and Forecasting Ocean Waves by Means of Wave Spectra and Statistics*. U.S. Department of the Navy Hydrographical Office Publications No. 603, 284p.
- SHERMAN, D.J. and GREENWOOD, B., 1986. Determination of wave angle in shallow water. *Journal of Waterway, Port, Coastal and Ocean Engineering*, 112, 129–139.
- SIMPSON, J.E., 1994. *Sea Breeze and Local Wind*. New York: Cambridge University Press, 234p.
- SONU, C.J.; MURRAY, S.P.; HSU, S.A.; SUHAYDA, J.N., and WADDELL, E., 1973. Sea breeze and coastal processes. *EOS, Transactions American Geophysical Union*, 54, 820–833.
- THORNTON, E.B. and GUZA, R.T., 1983. Transformation of wave height distribution. *Journal of Geophysical Research*, 88, 5925–5938.